Phantom studies and clinical application of high resolution, image reconstruction using ^{18}F-Fluoromethylcholine PET/CT for prostate cancer

Anna Zielinski* MD,
Florian F. Behrendt* MD,
Frederik A. Verburg MD,
Felix M. Mottaghy MD,
Thomas Krohn MD
** both authors contributed equally to this work.*

Department of Nuclear Medicine, RWTH University Hospital Aachen

Keywords: PET/CT
- High resolution
- Prostate cancer
- ^{18}F-methylcholine

Correspondence address:
Thomas Krohn, MD
RWTH University Hospital Aachen,
Department of Nuclear Medicine
Pauwelsstraße 30
52074 Aachen, Germany
Tel: +49-241-80 88740
Fax: +49-241-80 82520
E-mail: tkrohn@ukaachen.de

Received:
20 August 2014
Accepted revised:
29 September 2014

Abstract

The aim of this study is to evaluate the impact of a high resolution (HR) image reconstruction with a voxel size of 2mm in comparison to the most routinely used standard reconstruction with 4mm voxels in patients suffering from prostate cancer having undergone ^{18}F-methylcholine PET/CT. *Phantom studies were performed* using a Jaszczak phantom and a custom made phantom containing small hot lesions (size 2-10mm). Clinical evaluation was performed on PET/CT scans of 50 patients. Images were reconstructed with 4mm and 2mm voxel size and analyzed quantitatively using AMIDE and MATLAB. Clinical images were judged by two observers concerning TNM staging, image quality and the correlation of PET and CT data. *Phantom studies revealed* increased SUVmean and SUVmax values in the HR images ($P<0.01$). The lower detection limit was approximately 3mm in the HR and 4-5mm in the conventional images. Lower FWHM values were found in the HR images. No significant difference was found concerning the image quality and the correlation of PET and CT (each $P>0.5$). For both reconstructions, a comparable total amount of lesions was reported ($P>0.5$) with no impact on the TNM staging. *In conclusion*, the HR PET reconstruction provides semi-quantitative advantages in the sense of an improved lower detection limit and increased semi-quantitative tumour-to-background ratios. In the setting of choline PET/CT for prostate cancer the high resolution reconstruction could be implemented clinically as there are no relevant qualitative differences between this and the conventional image resolution in terms of image quality, assessment confidence and lesion identification rate.

Hell J Nucl Med 2014: 17(3): 194-199 *Epub ahead of print: 12 November 2014* *Published online: 22 December 2014*

Introduction

Common reconstruction algorithms for positron emission tomography (PET) images in the context of combined imaging with computed tomography (PET/CT) often generate isotropic voxels with a size of 4mm. However, image reconstruction with a higher resolution, e.g. with 2mm voxel size, is technically possible. Although the clinical impact of such high-resolution PET image reconstruction algorithms has not yet been sufficiently evaluated, it is conceivable that this might be beneficial for the detection of small tumour lesions. This could have an impact on the staging of various forms of cancer.

One such tumour entity is prostate cancer (PCa), which is the most common cancer in men, comprising 25.4% of all male cancer cases. It is one of the leading causes of cancer deaths of men in Europe [1, 2]. In recent years combined ^{18}F-methylcholine (^{18}F-FMC) PET and X-ray computed tomography (PET/CT) has increasingly been used for imaging in prostate cancer, especially for the localization of suspected recurrent disease [3]. Choline is one of the most sensitive tracers for PCa lesions in the prostate itself with a reported sensitivity of 66%-81% and a specificity of 81%-87% in combined PET/CT [4-6]. Therefore, ^{18}F-FMC PET/CT can be considered as a state-of-the-art imaging method in PCa for tumour staging and also for the planning of radiation treatment [7-9].

Prostate cancer often leads to small lymph node metastases in the pelvis. The distribution of these metastases usually follows typical patterns and the presence of metastases has a significant impact on tumour treatment. As the pelvic region is not prone to relevant motion artifacts, an accurate estimation of radiotracer uptake in small lesions is possible. This is in contrast to e.g. small pulmonary nodules, in which the tracer uptake is often underestimated due to motion artifacts caused by breathing.

The aim of the present study was to investigate the impact of a high resolution re-

construction on semi-quantification of PET images in phantom studies and to evaluate the impact of the increased resolution reconstruction on qualitative assessment of PET scans, using ^{18}F-FMC PET/CT for PCa as an example.

Subjects, materials - methods

Patients

This retrospective study comprises 50 men suffering from PCa, with a mean age of 70 (+/- 26) years, who were examined with ^{18}F-FMC PET/CT between January and November 2011. Indications for ^{18}F-FMC PET were primary staging after a positive prostate biopsy (n=19), tumour localization in patients with an increasing serum level of prostate specific antigen (PSA) (n=24) or a follow-up evaluation of PCa for planning of further treatment (n=7). The median PSA level in the population of included patients was 12.7ng/mL (range 0.3-142.8).

Image acquisition

Imaging was performed on a Gemini TF 16 PET/CT scanner (Philips Medical Systems, Best, The Netherlands) which consists of a 16-slice CT scanner and a fully three-dimensional, time-of-flight (TOF) capable PET scanner. The PET scanner is constructed with 28 flat modules each consisting of a 23×44 array of 4x4x22mm lutetium-yttriumoxyorthosilicate (LYSO) crystals placed in a full ring. The scanner bore has a diameter of 71.7cm with active transverse and axial field of views (FOV) of 57.6 and 18cm, respectively for both the PET and the CT component.

All patients received at least 2MBq ^{18}F-FMC/kg body weight (258±49MBq ^{18}F-FMC, range: 162-371MBq) 45-60min prior to the PET scan in accordance with the German Federal Law on the Compassionate Use of Medical Substances. Each patient gave written informed consent for the ^{18}F-FMC PET/CT examination.

Patients were scanned in cranio-caudal orientation with their arms raised to decrease beam-hardening artefacts. First a low dose CT from the base of the skull to the upper thigh was performed without contrast medium for attenuation correction purposes (scanning parameters: collimation 16×1.5mm; pitch 0.812; rotation time 0.4sec; effective tube current–time product of 30mAs; tube voltage of 120kVp). Computed tomography scans were used for attenuation correction as well as for anatomical correlation. Following the CT, a PET scan was performed with an acquisition time of 1.5min per bed position. Data were collected in list mode for all coincident events along with their time stamps. For each patient, 9 to 11 bed positions were acquired.

Image reconstruction

Slices of 4mm thickness (pixel size 4×4mm) were reconstructed using the proprietary iterative BLOB-OS-TF algorithm (number of iterations=3, number of subsets=33) which is provided by the scanner's manufacturer. This results in a matrix size of 144x144 voxels per slice. In the same way, slices of 2mm thickness (pixel size 2x2mm) were reconstructed generating a matrix size of 288x288 voxels.

Phantom measurements

In the first phantom experiment, an elliptical shape modified NEMA/IEC phantom (17cm wide, 30cm deep) was used with a total background volume of 9.98 liters. It contains six hollow spheres with volumes of 0.5, 1.0, 2.0, 5.5, 11 and 20mL, respectively, which can be filled with radioactivity to simulate hot spots. The phantom was filled with ^{18}F with a total activity of approximately 60MBq. Sphere-to-background activity ratios in two different measurements were 4:1 and 8:1, respectively, to simulate clinically realistic tumour-to-background ratios. Matching the patient studies, image acquisition was performed with an acquisition time of 90sec in one bed position.

For the assessment of the lower detection limit of small lesions, in a second experiment a custom phantom with smaller volumes was constructed. It consisted of an acrylic glass bar with dimensions of 10x15mm and a length of 300mm. A total of nine cylindrical bore holes were placed inside the bar with diameters decreasing from 10 to 2mm in steps of 1mm; the depth of each hole equals its diameter. After filling the bore holes with radioactivity the phantom was closed with adhesive tape so that it could be easily immersed into a basin containing the background activity. Figure 1 and Table 1 summarize the dimensions and characteristics of the custom phantom. The custom phantom was filled with ^{18}F at an activity concentration of approximately 10kBq/mL. Image acquisition parameters were similar to the patient studies; two different acquisitions were performed without background activity and with a hot spot-to-background ratio of 8:1, respectively.

Table 1. *Dimensions of the custom phantom*

Diameter [mm]	Depth [mm]	Volume [mL]
10	10	0.79
9	9	0.57
8	8	0.40
7	7	0.27
6	6	0.17
5	5	0.10
4	4	0.05
3	3	0.02
2	2	0.01

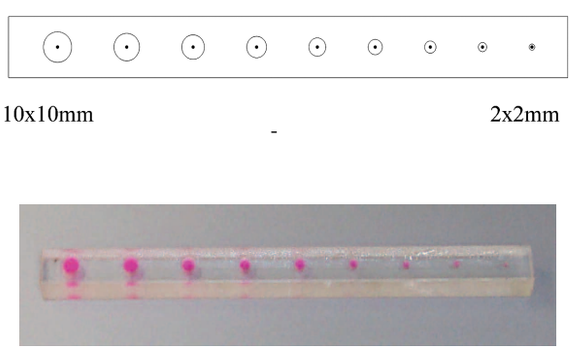

Figure 1. Custom phantom with small volumes. For a better visualization, the phantom bore holes are filled with a purple colorant in addition to the radioactivity.

Semi-quantitative measurements

To illustrate the detectability of the lesions we made a comparative line-profile analysis for each contrast using the open-source software tool AMIDE [10]. By means of the curve fitting toolbox from MATLAB 2009b (The Math Works inc., Natick, Massachusetts, USA) the resulting data sets (position and corresponding count rate) were fitted, based on a Gaussian model: $f(x)= a * e ^{[-(x-b)^2/2*c^2]}$. With the resulting c from the first equation the full-width at half-maximum (FWHM) of each curve was calculated using the formula: FWHM=2 * [(2 * ln 2) ^1/2] * c, where the FWHM value equates to the spatial resolution.

For a semi-quantitative comparison of the standard reconstruction with the high resolution PET reconstruction, the images were compared regarding the ^{18}F-FMC standard uptake value (SUV). The Philips PET/CT viewer (Extended brilliance™ Workspace, EBW™, V4.5.3.40140, Philips Medical Systems, Best, NL) was used to determine regions of interests (ROI) which were placed in five standard localizations (lumbar spine, lung, mediastinal blood pool, liver, psoas muscle) on the transverse PET images. The circular ROI had a diameter from 15 to 60mm.

For all ROI, the mean and maximum SUV was measured. The difference between the SUV for the standard vs. high resolution PET images was calculated as a percentage. The images of the Jaszczak phantom were analyzed in the same way as the patient studies; SUV inside the hot spheres and the background SUV were measured using ROI. The ROI diameters equaled the phantom sphere diameters.

Semi-qualitative image analysis

The reconstructed high resolution images and the original images were judged by two experienced board certified nuclear medicine physicians. All images were evaluated on the Philips PET/CT viewer. The physicians evaluated the images in a random order and were blinded to clinical data and reconstruction parameters. For anatomical correlation, each PET/CT was supplemented with the corresponding low-dose CT.

The images were reviewed with regard to designation of lesions, image quality, confidence in clinical interpretation and comparability with the CT-data.

For the lesion detectability five regions (lymph nodes in inguinal, iliac, perirectal and periaortal regions as well as the skeleton from the skull base to the thigh) were examined. The regions were chosen as they represent sites often affected by PCa metastases. A score was assigned to each region: negative, no cancer (1), ambiguous lesion (2), probably positive lesion (3), positive, i.e. certainly malignant lesion (4). The number of lesions in every region was recorded. The subjective image quality was graded in a 5-point rating as non-diagnostic (1), poor (2), moderate (3), good (4), or excellent (5). This value includes aspects like relative resolution, contrast, sharpness and subjective overall image quality. Furthermore each reader graded the images in terms of confidence in making a clinical interpretation and in the subjective ease of correlation of lesions with the CT-scan with a five-point score: excellent (1), good (2), fair (3), poor (4) and very poor (5).

For each patient data set, an N and M staging was assigned according to the TNM-AJCC system. In case of differences in TNM staging between the two observers, the observers conferred to reach a consensus.

Statistical analysis

All statistical analyses were carried out using SPSS 20 (IBM corp., Somers, USA).

Paired t-tests were conducted for comparison of SUVmean and SUVmax between the different reconstructions in the phantom studies. The two-sided nonparametric paired Wilcoxon test was used to compare the number of lesions for each anatomical region. $P<0.05$ was deemed to indicate statistical significance. Interobserver agreement for N and M staging was evaluated by kappa statistics (poor agreement, $\kappa=0$; slight agreement, $\kappa=0.01$-0.20; fair agreement, $\kappa=0.21$-0.40; moderate agreement, $\kappa=0.41$-0.60; good agreement, $\kappa=0.61$-0.80; and excellent agreement $\kappa=0.81$- 1.0).

Results

Phantom studies

Regarding the Jaszczak phantom, the SUVmean values obtained from the high resolution images were significantly higher for each of the hot spheres, no matter which size, for each contrast (all $P<0.0001$). The arithmetic mean of the difference between the ROI in the regular and the high resolution PET/CT-images was 21.1% for the 4:1 contrast and 17.8% for the 8:1 contrast. The SUVmax values were also significantly higher. Table 2 summarizes the SUV measured under the different conditions. The background SUVmean showed no significant difference between the standard vs. the high resolution reconstruction for each contrast ratio. See Figure 2 for an example of the phantom images.

The FWHM values calculated by a curve fitting performed in MATLAB after generating line profiles with AMIDE were

***Table 2**. Count rates obtained from the phantom studies. Values are given as SUVmean*

Phantom setup	SUVmean 2mm	4mm	Delta [%]	P
2mL, 1:4	2.4	1.7	41.18	<0.0001
5.5mL, 1:4	2.5	2.2	13.64	<0.0001
11mL, 1:4	2.6	2.4	8.33	<0.0001
2mL, 1:8	4.8	3.8	26.32	<0.0001
5.5mL, 1:8	5.4	4.4	22.73	<0.0001
11mL, 1:8	4.8	4.6	4.35	<0.0001

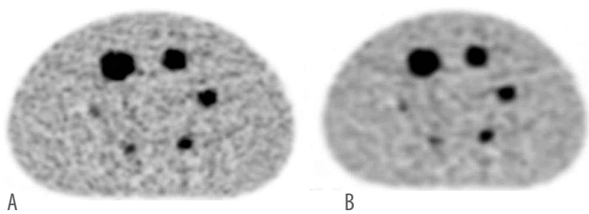

Figure 2. Jaszczak phantom images. Contrast ratio 4:1, Acquisition time 90sec. A: high resolution reconstruction, B: conventional reconstruction.

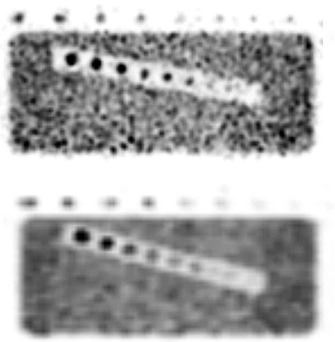

Figure 3. Lower detection limits obtained from the studies with the custom phantom. The smallest clearly delineable volume is approx. 3mm for the high resolution (left image) and approx 4-5mm for the conventional reconstruction (right image).

significantly lower for the high resolution image reconstruction in comparison to the conventional resolution of 4mm voxel-size for all contrasts and sphere sizes. For example, the FWHM calculated for the 5.5mL sphere at a contrast ratio of 1:4 was 25mm in the conventional and 22.4mm in the high resolution reconstruction.

The visual analysis of the images acquired using the custom phantom revealed a lower detection limit of approximately 3mm for the high resolution reconstruction and a slightly higher detection limit of approximately 4-5mm for the conventional reconstruction (Fig. 3). In general, small volumes can be more clearly delineated in the high resolution images.

Patient data

The SUVmean values in the high resolution images were significantly higher than those in the routinely used 4mm voxel size images (P<0.0001). SUVmean values were significantly higher for the ROI measurements of the pelvic muscular tissue (arithmetic mean of the differences of 2mm compared to 4mm +0.114), the tumour lesions (+0.759), the liver (+0.674) and the first lumbar vertebra (+0.166), whereas there SUVmean values were significantly lower for the measurements in the lung (-0.05), each P<0.01.

***Table 3**. Uptake of different regions in the patient measurements. Values as SUVmean±SD*

Organ	SUVmean			
	2mm	4mm	Delta	P
Lung	0.56±0.17	0.61±0.17	- 8.20%	<0.0001
Liver	8.49±2.19	7.82±2.03	+ 8.57%	<0.0001
Lesion	3.87±1.76	3.09±1.41	+ 25.24%	<0.0001
Lumbar vertebrae	2.38±0.51	2.21±0.43	+ 7.69%	<0.0001
Mediastinal blood pool	0.60±0.14	0.59±0.12	+ 1.69%	P=0.1797
M. psoas	1.19±0.81	1.07±0.59	+ 11.21%	<0.0001

Finally, SUVmean values for the mediastinal background uptake (P=0.18) did not differ significantly with a mean difference of +0.01.

Results for the SUVmean measurements for the different PET reconstructions are given in Table 3.

Additionally, an analysis of the liver and lesion to background ratio revealed significant increase in those values in the 2mm reconstructions compared to the 4mm PET/CT (both P<0.0001). The liver-to-background ratio for the high resolution was 15.22% higher than in the standard images, whereas there was an increase of 33.19% for the lesion-to-background values in the high resolution images (each P<0.001).

Semi-qualitative image analysis

In 94 of 100 data sets (two per patient) the assessment of the nodal staging was concordant between the two observers. For the high resolution reconstruction, the two observers reported an identical nodal staging in 48/50 (kappa=0.92) and for the conventional reconstruction in 46/50 cases (kappa=0.839). For the presence of distant metastases, the observers reported concordant results in 46/50 cases (kappa=0.703) for the high resolution and in 45/50 data sets (kappa=0.646) for the conventional 4x4mm reconstruction. In cases with a discrepant finding for TNM staging consensus reading was performed.

No significant differences were found concerning the subjective image quality (observer 1: 3.78 (2mm) vs. 3.76 (4mm), P=0.830; observer 2: 3.34 (2mm) vs. 3.28 (4mm), P=0.622),

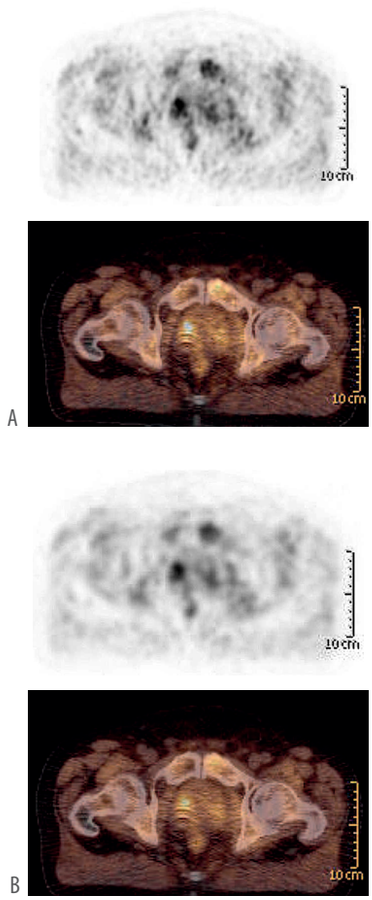

Figure 4. PET/CT images of a patient with recurrent prostate cancer. A: high resolution reconstruction, B: conventional reconstruction.

the subjective confidence in making a clinical decision (observer 1: 2.16 vs. 2.20, P=0.617; observer 2: 2.56 vs 2.48; P=0.529) and the subjective ease of correlation of PET findings with the low dose CT (observer 1: 2.14 vs. 2.20, P=0.439; observer 2: 2.64 vs. 2.58, P=0.635).

A comparable total number of metastatic lesions were found by the two observers. A total of 110 metastases were reported for the high resolution and 112 metastases for the conventional reconstruction by observer 1, (P=0.223), whereas observer 2 reported 113 and 112 metastases, respectively (P=0.932). An analysis of inter-observer variability revealed no significant differences for the high resolution reconstruction (P=0.734) or the conventional 4mm reconstruction (P=0.223). See Figure 4 for PET/CT images reconstructed with conventional and high resolution reconstruction.

Discussion

The present study shows that although a high resolution PET reconstruction allows for a more precise semi-quantitative reconstruction and assessment of PET images, the clinical impact of such high resolution reconstruction appears to be modest in the sense that clinical, non-semi-quantitative assessment of images changes little.

Our phantom studies revealed that the high resolution reconstruction theoretically allows for improved lesion detection as a. a decrease of the lower detection limit for lesion size and b. an increased lesion-contrast as well as c. a raised measured radioactivity concentration within the lesions both in vivo and in phantoms. Therefore, at least in theory the high resolution reconstruction is superior for the visualization of small lesions in line with the results of a study by Rodrigues et al (2009), who compared head/neck (HN) PET images reconstructed with a conventional and a high resolution algorithm from 44 patients with head and neck tumours [11]. The HN PET/CT high resolution protocol demonstrated a better performance in detecting cervical lymph node metastases. The greatest advantage was observed in the detection of small positive lymph nodes <15mm (4-fold increase in nodal detection compared to the standard reconstruction).

For prostate cancer, Beheshti et al (2010) described a sensitivity of 66% and specificity of 96% in lymph node metastases ≥5mm for preoperative ^{18}F-FMC PET/CT imaging, but a total sensitivity of 45% and specificity of 96% for all lymph node metastases (including those <5mm) as compared to histological findings [12]. For ^{18}F-FDG PET/CT in melanoma, Crippa et al (2000) described a sensitivity of 100% for the detection of nodal metastases larger than 1cm, but only 23% for nodal metastases ≤5mm as compared to the postoperative histopathology results [13].

The cause for the limited sensitivity in the detection of especially smaller lymph node metastases in the above studies probably lies in the limited spatial resolution attained with current standard reconstruction algorithms, which is about 7-8mm [14, 15].

The assessment of the images by two independent investigators revealed that in general both reconstruction algorithms generate comparable clinical results concerning the image quality, a detailed tumour characterization and staging. A study from Yamamoto et al (2007) concerning head and neck cancer [16] had similar results. In 55 patients they did not find a significant difference in the diagnostic performance of the standard and dedicated high resolution head-and-neck PET protocol regarding the clinical lesion detection. They also based their information on phantom measurements and like in our study found a significant improvement in small lesion detection with a higher signal-to-background ratio for all spheres in the high-resolution PET images regarding the standard PET images.

Yamamoto et al (2007) extended the measure time for the high resolution images up to 8min per bed position to avoid increased noise. Remarkably however this appears not to be necessary: in the present study we could not lengthen acquisition time as we reconstructed images from scans that were acquired before in regular clinical care. Nonetheless, even with a standard acquisition time we did not find any significant changes in the subjective image quality or the subjective confidence in making a decision and correlation with the CT.

The retrospective nature of the present study is also its weakness: we had to contend with datasets that were already acquired and were unable to vary factors such as acquisition time or administered activity in order to further study the influence of such variables. However, considering that even in this setting we found no semi-qualitative differences between the algorithms with acquisition parameters that are not optimized for the high resolution algorithm, the influence of such variables was likely minimal. In a further limitation of our study, a recognition bias concerning lesion identification cannot be ruled out completely; we did however try to minimize it by blinding the observers to clinical and reconstruction data and putting the data in a random order which was different for each observer. Furthermore we had a lack of histological verification, thus we could neither define the sensitivity nor the specificity of the resulting clinical findings. Thus, further research including histological confirmation of scan results appears warranted; especially in the case of smaller lymph node metastases histological lymph node analyses could contribute to optimization of the high resolution reconstruction algorithm to help better identify such metastases on PET/CT.

A likely explanation for the lack of an increase in the number of lesions detected might be the physiologic distribution of ^{18}F-FMC. Considering that ^{18}F-FMC is also taken up by e.g. the digestive system, it is quite likely that very small lesions are obscured by relevant background activity uptake in a patient. Furthermore, we had no gold standard to compare with, we have thus far been unable to calibrate the uptake in very small lesions against findings on pathology examination of such lesions. Here a clinical follow up study could perhaps yield additional information.

The lack of a clinical difference between the two reconstruction algorithms in many respects will work in favour of the high resolution reconstruction, although a disadvantage of the high resolution reconstruction is that twice as much transaxial slices are generated making the clinical evaluation of the images more time-consuming.

Considering that computing power is hardly a problem these days, the more computing intensive high resolution

can be used in clinical practice without markedly changing visual imaging assessment which would require re-training on the side of the assessing physicians. However, in cases where were semi-quantitative assessment may be essential, such as in oncological drug evaluation studies, the high resolution reconstruction will allow for a more accurate semi-quantification.

In conclusion, the 2mm high resolution PET reconstruction especially provides semi-quantitative advantages in the sense of an improved lower lesion size detection limit, better image resolution and increased semi-quantitative tumour-to-background ratios. In the setting of ^{18}F-FMC PET/CT for prostate cancer this reconstruction method could be implemented clinically as there are no relevant semi-qualitative differences between this and the conventional reconstruction algorithm in terms of lesion identification rate, image quality and assessment confidence.

Acknowledgement
This study was supported by a grant from Philips Medical Research, Aachen, Germany.

The authors declare that they have no conflicts of interest.

Bibliography

1. Malvezzi M, Bertuccio P, Levi F et al. European cancer mortality predictions for the year 2012. *Ann Oncol* 2012; 23: 1044-52.
2. Bantis A, Vasiliou O. Prostate cancer incidence, mortality, total and free prostate specific antigen. *Hell J Nucl Med* 2009; 12: 106-9.
3. Emonds KM, Swinnen JV, Mortelmans L, Mottaghy FM. Molecular imaging of prostate cancer. *Methods* 2009; 48: 193-9.
4. Cook GJ, Fogelman I. The role of positron emission tomography in the management of bone metastases. *Cancer* 2000; 88: 2927-33.
5. Muller J, Schrader M, Schrader AJ et al. Value of positron emission tomography in urological neoplasms: more form than substance? *Urologe A* 2012; 51: 331-40.
6. Reske SN, Blumstein NM, Neumaier B et al. Imaging prostate cancer with ^{11}C-choline PET/CT. *J Nucl Med* 2006; 47: 1249-54.
7. Schoder H, Larson SM. Positron emission tomography for prostate, bladder, and renal cancer. *Semin Nucl Med* 2004; 34: 274-92.
8. Pinkawa M, Eble MJ, Mottaghy FM. PET and PET/CT in radiation treatment planning for prostate cancer. *Expert Rev Anticancer Ther* 2011; 11: 1033-9.
9. Skoura E, Datseris IE. The use of ^{18}F-fluorothymidine and ^{18}F-fluorocholine in imaging with positron emission tomography. *Hell J Nucl Med* 2010; 13: 88-90.
10. Loening AM, Gambhir SS. (2003) AMIDE: a free software tool for multimodality medical image analysis. *Mol Imaging* 2003; 3: 131-7.
11. Rodrigues RS, Bozza FA, Christian PE et al. Comparison of Whole-Body PET/CT, Dedicated High-Resolution Head and Neck PET/CT, and Contrast-Enhanced CT in Preoperative Staging of Clinically M0 Squamous Cell Carcinoma of the Head and Neck. *J Nucl Med* 2009; 50: 1205-13.
12. Beheshti M, Imamovic L, Broinger G et al. ^{18}F Choline PET/CT in the Preoperative Staging of Prostate Cancer in Patients with Intermediate or High Risk of Extracapsular Disease: A Prospective Study of 130 Patients. *Radiology* 2010; 254: 925-33.
13. Crippa F, Leutner M, Belli F et al. Which kinds of lymph node metastases can FDG-PET detect? A clinical study in melanoma. *J Nucl Med* 2000; 41: 1491-4.
14. Husarik DB, Miralbell R, Dubs M et al. Evaluation of ^{18}F-choline PET/CT for staging and restaging of prostate cancer . *Eur J Nucl Med Mol Imaging* 2008; 35: 253-63.
15. Conti M. State of the art and challenges of time-of-flight PET. *Phys Med* 2009; 25: 1-11.
16. Yamamoto Y, Wong TZ, Turkington TG et al. Head and Neck Cancer: dedicated FDG PET/CT protocol for detection- phantom and initial clinical studies. *Radiology* 2007; 244: 263-72.